

# Cytotoxicity Effects of Curcumin Loaded on Chitosan Alginate Nanospheres on the KMBC-10 Spheroids Cell Line

This article was published in the following Dove Press journal:  
International Journal of Nanomedicine

Elham Afzali<sup>1</sup>  
Touba Eslaminejad<sup>1</sup>  
Seyede Elmira Yazdi  
Rouholamini<sup>2</sup>  
Mariam Shahrokhi-Farjah<sup>2</sup>  
Mehdi Ansari<sup>3</sup>

<sup>1</sup>Pharmaceutics Research Centre, Institute of Neuropharmacology, Kerman University of Medical Sciences, Kerman, Iran; <sup>2</sup>Physiology Research Centre, Institute of Basic and Clinical Physiology Sciences, Kerman University of Medical Sciences, Kerman, Iran; <sup>3</sup>Department of Drug and Food Control, Faculty of Pharmacy, Kerman University of Medical Sciences, Kerman, Iran

**Purpose:** Breast cancer is one of the most lethal types of cancer in women. Curcumin showed therapeutic potential against breast cancer, but applying that by itself does not lead to the associated health benefits due to its poor bioavailability, which appears to be primarily due to poor absorption, rapid metabolism, and rapid elimination. Moreover, poor water solubility of curcumin causes accumulation of a high concentration of curcumin and so decrease its permeability to the cell. Many strategies are employed to reduce curcumin metabolism such as adjuvants and designing novel delivery systems. Therefore, in this study sodium alginate and chitosan were used to synthesize the hydrogels that are known as biocompatible, hydrophilic and low toxic drug delivery systems. Also, folic acid was used to link to chitosan in order to actively target folate receptors on the cells.

**Methods:** Chitosan- $\beta$ -cyclodextrin-TPP-Folic acid/alginate nanoparticles were synthesized and then curcumin was loaded on them. Interaction between the constituents of the particles was characterized by FTIR spectroscopy. Morphological structures of samples were studied by FE-SEM. Release profile of curcumin was determined by dialysis membrane. The cytotoxic test was done on the Kerman male breast cancer (KMBC-10) cell line by using MTT assay. The viability of cells was detected by fluorescent staining. Gene expression was investigated by real-time PCR.

**Results:** The encapsulation of curcumin into nano-particles showed an almost spherical shape and an average particle size of 155 nm. In vitro cytotoxicity investigation was indicated as dose-response reaction against cancer breast cells after 24 h incubation. On the other hand, in vitro cell uptake study revealed active targeting of CUR-NPs into spheroids. Besides, *CXCR4* expression was detected about 30-fold less than curcumin alone. The CUR-NPs inhibited proliferation and increased apoptosis in spheroid human breast cancer cells.

**Conclusion:** Our results showed the potential of NPs as an effective candidate for curcumin delivery to the target tumor spheroids that confirmed the creatable role of folate receptors.

**Keywords:** spheroids cell, curcumin, nanospheres, cytotoxicity, chitosan, alginate

## Introduction

The abnormal proliferation of cells leads to cancer disease.<sup>1</sup> The most common invasive cancer in women is breast cancer and it is also the second main cause of cancer death in women, after lung cancer.<sup>2</sup> 3D spheroid cells are formed by cancer cells that include a central necrotic core with peripheral proliferating cells.<sup>1</sup> Research has shown that multicellular tumor spheroids are able to predict the in vivo drug efficacies.<sup>1</sup> Anticancer drugs showed many limitations, eg, poor water solubility and low targeting efficiency.<sup>3</sup>

Correspondence: Mariam Shahrokhi-Farjah; Touba Eslaminejad  
Tel +983431325243  
Fax +983431325003  
Email M\_Shahrokhi@KMU.ac.ir;  
t\_eslami@kmu.ac.ir

Therefore, new delivery systems that could solve these problems are needed. Curcumin as a polyphenol that is extracted from the rhizomes of the *Curcuma longa* plant.<sup>4</sup> Curcumin showed various pharmacological effects including those of apoptotic, anti-proliferative, anti-oxidant, and anti-angiogenic properties and anticancer properties with no significant side effects.<sup>5</sup> Recent findings showed the great activities of curcumin against many types of cancer, eg, melanoma, breast and prostate cancers.<sup>6</sup> There are many reports about loading curcumin as a drug on polymers such as encapsulation into nano-gels.<sup>6</sup> Hydrogels that are synthesized by using natural polymers, known as biocompatible, hydrophilic and low toxic drug delivery systems.<sup>7</sup> Moreover, hydrogels are widely syntheses of biopolymers such as chitosan and alginate.<sup>8</sup> They are typically used for encapsulating hydrophilic drugs.<sup>8</sup> Sodium Alginate is a polymer that consisted of l-guluronic acid and d-mannuronic acid.<sup>9</sup> Chitosan is a polysaccharide that derived from chitin and it is widely utilized as cationic ligand.<sup>10</sup> Also chitosan, alginate and a combination of them were used as targeted nanoparticles such as coating the magnetic particles or grafting specific ligands.<sup>11,12</sup> For example, sodium alginate grafted magnetic nanospheres were used as a controlled drug delivery system for Cisplatin in the in vitro environment.<sup>13</sup> Moreover, sodium alginate was used as surface modifier on magnetic nanoparticles containing gentamicin for antibacterial targeting therapy.<sup>14</sup> In addition, superparamagnetic nanoparticles coated by alginate/chitosan/ $\beta$ -cyclodextrin were used to purify  $\alpha$ -amylase enzyme.<sup>15</sup> Targeted nanoparticles have been used in drug delivery to cancer cells because of their characteristics. Magnetic nanoparticles are used because of directing and controlling by external magnetic field.<sup>16,17</sup> In the present study, drug delivery systems were designed according to the cell's characteristics (folate receptors) to have a targeted system. Folic acid was used to link to chitosan in order to confer it redox responsiveness and active targeting of folate receptors.<sup>18</sup> Since expression of *CXCR4* is enhanced in metastasized breast cells carcinoma.<sup>19</sup> So, the main aim of this study was to encapsulate the curcumin into nanospheres to enhance curcumin efficacy against cancer cells through evaluation of their viability (%) and the *CXCR4* gene expression.

## Materials and Methods

Dulbecco's modified Eagle's medium (DMEM), fetal bovine serum (FBS), Dulbecco's phosphate buffered saline (PBS), penicillin/streptomycin, and trypsin were obtained from Gibco (Carlsbad, CA, USA); Annexin V-FITC kit was purchased from BD Biosciences (San Jose, CA, USA).

Curcumin was obtained from Sigma Chemicals (Perth, Australia). Thiazolyl Blue Tetrazolium Bromide (MTT) cell viability dye, Propidium iodide (PI), Hoechst 33,342 (H), Dimethyl sulfoxide (DMSO), folic acid, polyethylene glycol (PEG), chitosan (low molecular weight),  $\beta$ -cyclodextrin, alginate, and tripolyphosphate (TPP) were purchased from Sigma-Aldrich Co., (St. Louis, MO, USA). All other materials used in this study were from domestic providers at analytical grade. KMBC-10 (Kerman male breast cancer) cells were obtained from patients according to protocol approved by Institutional Review Board of Kerman University of Medical Sciences, Kerman, Iran (IR.KMU.REC. approval number 1398.025) and all patients gave written informed consent to participate. The study was performed in accordance with the Declaration of Helsinki and standards of good clinical practice.

## Preparation of Chitosan/ $\beta$ -Cyclodextrin /TPP-Folic Acid/Alginate/Curcumin (CS/ $\beta$ -CD/TPP-Folic Acid/Alg-CUR)

CS/ $\beta$ -CD/TPP/CUR nanoparticles were synthesized by ionotropic gelification as previously described.<sup>20</sup> First of all, acidified chitosan was mixed with 1 mL of PEGylated curcumin (PEG 6000, 50%) and then the corresponding quantity of the TPP solution (1.5 mg/mL) was added drop-wised at a final volume of 1 mL.<sup>21,22</sup> Folic acid (1 mM) was dissolved in aqueous solution containing 10 mM Tris-HCl buffer (pH 7.4) and conjugated with CS/ $\beta$ -CD/TPP/CUR solution (40  $\mu$ M) at final volume of 3 mL stirring magnetically for 24 h. Alginate suspension (10 mL) was slowly mixed with CS/ $\beta$ -CD/TPP/CUR/folic acid (3 mL). Then 0.5 mL of 100 mM CaCl<sub>2</sub> solution was added drop-wised into suspension (13 mL) and left to dry at room temperature under vacuum for 12 h.<sup>23</sup>

## Physical Characterization of Nanospheres

Fourier transform infrared spectroscopy (FTIR) was performed using FTIR-spectrometer (Bruker Optik GmbH, Ettlingen, Germany) to understand the interaction between the constituents of the particles. CS/ $\beta$ -CD/TPP-Folic acid/Alg, CS/ $\beta$ -CD/TPP-Folic acid/Alg-CUR samples were determined as KBr discs in (3500–500 cm<sup>-1</sup>).<sup>24</sup> Morphological structures of samples were studied by field emission scanning electron microscopy (FE-SEM) (Sigma, Carl Zeiss, Germany) at voltage of 20 kV after coating of each sample with a thin layer of gold for 5 min. Parameters such as size of nanoparticles and zeta potential were measured using

a Scattering Particle Size Analyzer (Malvern Instruments, Malvern, UK). Moreover, the images were analyzed by Image Ara software.

## Determination of Release Profile

Release of curcumin from nanoparticles was measured in phosphate-buffered saline (PBS), pH 5.8 at different time intervals. Samples were dialyzed by dialysis membrane (MWCO 12,000 Da) against PBS and free curcumin in the supernatant was quantified by (Optizen 3220UV, South Korea) instrument at absorbance at 430 nm.

## Formation of Spheroids

KMBC-10 (Kerman male breast cancer) cells were grown at 37 °C; 5% CO<sub>2</sub> in DMEM-F12 supplemented with 20 ng/mL EGF, 20 ng/mL BFGF and 1% penicillin/streptomycin solution and 10% FBS. Spheroids were formed from 10<sup>4</sup> cells in 96 wells plate during 7 days.<sup>25</sup> Then spheroids were investigated by observing under light microscopy (Nikon, Eclipse 80i; Tokyo, Japan).

## MTT Assay

MTT assay for cell culture was obtained after 24 h of treatment, the concentrations of nanospheres ranged by 15, 25, 35, 50, 65, and 75 were utilized in 3 replicates, incubated for 24 h more. 10 µL of MTT solution was added into each well and incubated for 4 h. After that the cell culture was centrifuged at 1500 g for 5 min. Then, 150 µL of media was harvested from each well. Plate was let to dry and added the 100 µL of DMSO and then the absorbance was read at 570–630 nm by immune absorbent assay (ELISA) (multi-mode reader, Synergy II; Bio-tek Instruments, USA).

## Fluorescent Staining in Spheroids

Fluorescent staining (Sigma-Aldrich) was used to detect viability of cells. Initially cells were treated with IC<sub>50</sub> concentration of nanospheres and then incubated for 24 h. After the treatment, spheroids were washed with PBS, the solution containing 5 µL from each one of 5 µM Hoechst 33,342 (H) and Propidium iodide (PI) was added, and the stained cells were assessed using a fluorescent microscopy (Nikon, Eclipse 80i) ( $\lambda_{\text{ex}}$ : 488 nm/ $\lambda_{\text{em}}$ : 530 nm).

## Apoptosis Assay

Apoptosis assay of cells were detected using an Annexin V-FITC apoptosis detection kit (BD Biosciences, Franklin Lakes, NJ, USA). Cells were seeded into 6-well plates

(concentration of 10<sup>5</sup> cells/well) and treated with IC<sub>50</sub> concentration of curcumin, CS/β-CD/TPP-Folic acid/Alg and CS/β-CD/TPP-Folic acid/Alg-CUR for 24 h and were washed twice with 200 µL PBS. Then, cells were centrifuged at 9300 g, and then incubated in the dark with 100 µL of binding buffer and stained with staining solution containing 5 µL Annexin V-FITC and 5 µL of PI at 37 °C for 20 min. Finally, cells were analyzed by flow cytometry (BD Biosciences), using 488 nm excitation and emission at 530–575 nm and after that data were plotted for Annexin V-FITC and PI.

## Real-Time PCR

Total RNA was extracted using TRIzol Reagent (Thermo Fisher Scientific, Waltham, MA, USA) and also cDNA synthesis was obtained using cDNA synthesis kit (*AccuPower<sup>®</sup> RocketScript<sup>™</sup>* Cycle RT PreMix Cat. No. K-2101, Bioneer). The thermal profile for the real-time PCR (Roche, Germany) was 95 °C for 10 min followed by 40 cycles of 95 °C for 30 s, 54 °C for 20 s, and 72 °C for 30s. The PCR product was detected as an increase in fluorescence with the ABI PRISM 7700 instrument (Thermo Fisher Scientific). PCR was performed with 12.5 mL of SYBR PCR master mixture, each of the primers (as shown in Table 1) at a concentration of 100 nM, and 1 mL of RT product in a total volume of 25 mL, normalized against 18S mRNA (Ambion Quantum RNATM 18S Universal Primers) and a standard curve constructed from serial dilutions of a purified *CXCR4* cDNA fragment.

## Statistical Analysis

Statistical comparison between curcumin, CS/β-CD/TPP-Folic acid/Alg and CS/β-CD/TPP-Folic acid/Alg-CUR treatment groups at different concentration were investigated using one-way ANOVA by SPSS software 15 for windows (SPSS Inc., Chicago, IL, USA) ( $p \leq 0.05$ ).

## Results

### Physical Characterization of Nanospheres

FTIR-spectrometer of CS, β-CD, TPP, ALG, CUR, Folic acid, CS-β-CD-TPP, CS/β-CD/TPP-Folic acid/Alg and CS/β-CD/TPP-Folic acid/Alg-CUR are shown in Figure 1. Wave numbers of β-CD at the range of 1029 cm<sup>-1</sup> present to C-O band (Figure 1A). The broad absorption band at 2902–3334 cm<sup>-1</sup> correspond to stretch O-H bond existing in the pure alginate and also the pure alginate spectrum

**Table I** Forward and Reverse Primers for *CXCR<sub>4</sub>* and 18S

Primer Name	Forward	Reverse
<i>CXCR<sub>4</sub></i> 18S	CTCCAAGCTGTCACACTCC GACAGGATGCAGAAGGAGAT	TCGATGCTGATCCCAATGTA TGCTTGCTGATCCACATCTG

assigned at the peaks at  $1028\text{ cm}^{-1}$  was illustrated in Figure 1B that related to C-O band. The peak characteristic of  $1629\text{ cm}^{-1}$  and  $3431\text{ cm}^{-1}$  are attributed to the chitosan (Figure 1C).<sup>26</sup> Moreover, the absorption band of CS at  $3431\text{ cm}^{-1}$  is attributed to the  $\text{NH}_2$  group. The intensity absorption band at  $1099\text{ cm}^{-1}$  dependent to C-O-C bond in PEG is indicated in Figure 1D. The spectra peak of free curcumin was demonstrated nearby  $3509\text{ cm}^{-1}$  beside (Figure 1E), this peak assigned to free hydroxyl group. Folic acid-chitosan conjugation was recorded by spectral shifting and intensity variations for the chitosan amide I band at  $1628\text{ cm}^{-1}$  while it is attributed to C=O stretch and amide II band about  $1728\text{ cm}^{-1}$  can be recognized to C-N and N-H stretch (Figure 1E). The FTIR spectrum of pure folic acid is characterized by  $2888$  and  $1467\text{ cm}^{-1}$  (Figure 1F). After complication the peaks of chitosan and  $\beta$ -cyclodextrin with alginate changed to  $1636\text{ cm}^{-1}$  (Figure 1G).<sup>27</sup> Nevertheless, an ionic interaction the carboxyl groups of alginate with amide groups of the chitosan formed the polyelectrolyte complex. Average size of CS/ $\beta$ -CD/TPP-Folic acid/Alg and CS/ $\beta$ -CD/TPP-Folic acid/Alg-CUR particles that was recorded by dynamic light scattering showed different measurement of  $115$  and  $371\text{ nm}$  at room temperature, respectively. Also, FE-SEM analysis of them confirmed that they were uniformly spherical (Figure 2A and B).

## Cytotoxic Effects of Nanospheres

Cells were treated in different concentration for  $24\text{ h}$  and the viability (%) of cells was measured by MTT assay. Data were performed from three independent experiments. Results showed that CS/ $\beta$ -CD/TPP-Folic acid/Alg-CUR nanospheres reduced the viability (%) of the KMBC-10 spheroids cells. The mean difference of cytotoxicity effect in curcumin, CS/ $\beta$ -CD/TPP-Folic acid/Alg and CS/ $\beta$ -CD/TPP-Folic acid/Alg-CUR treatment groups were significant at  $p < 0.05$  (Figure 3). Since curcumin is insoluble in water, when it is exposed to an aqueous medium in cell culture, increasing the concentration of curcumin leads to increased accumulation of curcumin. On the other hand, its permeability to the cell was decreased. The  $\text{IC}_{50}$  of CS/ $\beta$ -CD/TPP-Folic acid/Alg-CUR was  $0.38\text{ mg/l}$  (Figure 4.)

## Release Profile of Curcumin

The release pattern of curcumin is shown in (Figure 5). Data showed that  $0$ ,  $13$ ,  $19$ ,  $25$ ,  $88$  and  $93\%$  of the curcumin was released during  $0$ ,  $1$ ,  $2$ ,  $3$ ,  $16$  and  $24\text{ h}$ , respectively.

## Fluorescent Staining in Spheroids

KMBC-10 spheroids cells were treated by curcumin and CS/ $\beta$ -CD/TPP-Folic acid/Alg-CUR nanospheres, separately. The CS/ $\beta$ -CD/TPP-Folic acid/Alg-CUR nanospheres showed the high cytotoxicity effect at  $65\text{ }\mu\text{g/mL}$  compared to curcumin that showed no significant fluorescence (Figure 6).

## Apoptosis Assay of Nanospheres

Apoptosis analysis of curcumin, CS/ $\beta$ -CD/TPP-Folic acid/Alg and CS/ $\beta$ -CD/TPP-Folic acid/Alg-CUR showed  $6$ ,  $0$  and  $20\%$  of apoptotic cells at  $\text{IC}_{50}$  concentration (Figure 7).

## Real-Time RT-PCR Analyses

*CXCR<sub>4</sub>* expression was decreased in the CS/ $\beta$ -CD/TPP-Folic acid/Alg-CUR group and was recorded about  $30$ -fold lower than curcumin (Figure 8).

## Discussion

According to the results, the high percentage of the encapsulated curcumin in the CS/ $\beta$ -CD/TPP-Folic acid/Alg hydrogel nanospheres was adsorbed by spheroid cells, as confirmed by flow cytometric and gene expression analysis. Hydrogel nanoparticles showed the properties that each hydrogel and nanoparticle have separately. They are used widely in pharmaceutical sciences such as in targeted cell therapy and drug delivery systems. Drugs encapsulated in hydrogels are protected against environmental agents such as enzymes or pH changes.<sup>28</sup> Also, the stability of the nanoparticle, crystalline structure, size and agglomeration affect the toxicity and biological distribution of the nanoparticles in the in vivo environment.<sup>29</sup> Chitosan has been mainly utilized in the mixture of nanocomposites that chitosan was a cationic and emulsifier.<sup>30</sup> Besides, chitosan is applied for delivering hydrophobic drugs such as curcumin to cancer cells.<sup>31</sup> The results recorded show that curcumin alone has problems in



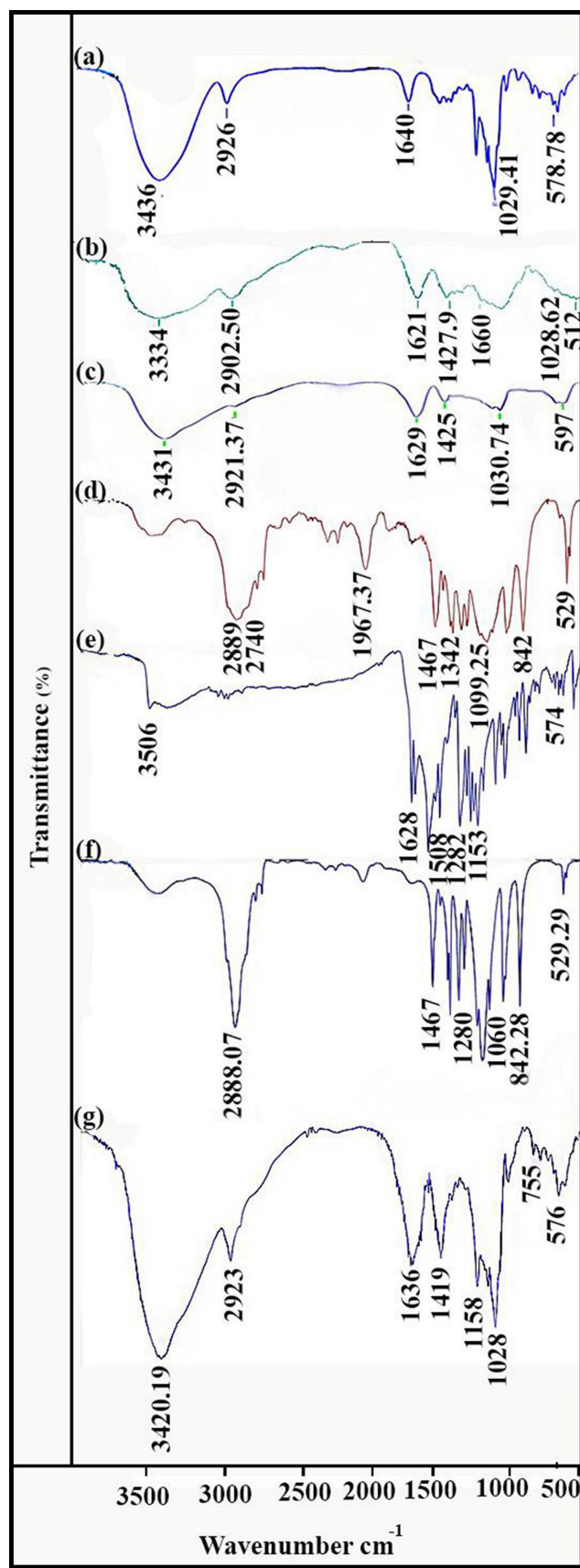


**Figure 1** FTIR spectra of the synthesized particles: (A)  $\beta$ -cyclodextrin, (B) Alginate, (C) Chitosan, (D) PEG, (E) Curcumin, (F) Folic acid, (G) CS/ $\beta$ -CD/TPP-Folic acid/Alg-CUR nanospheres.

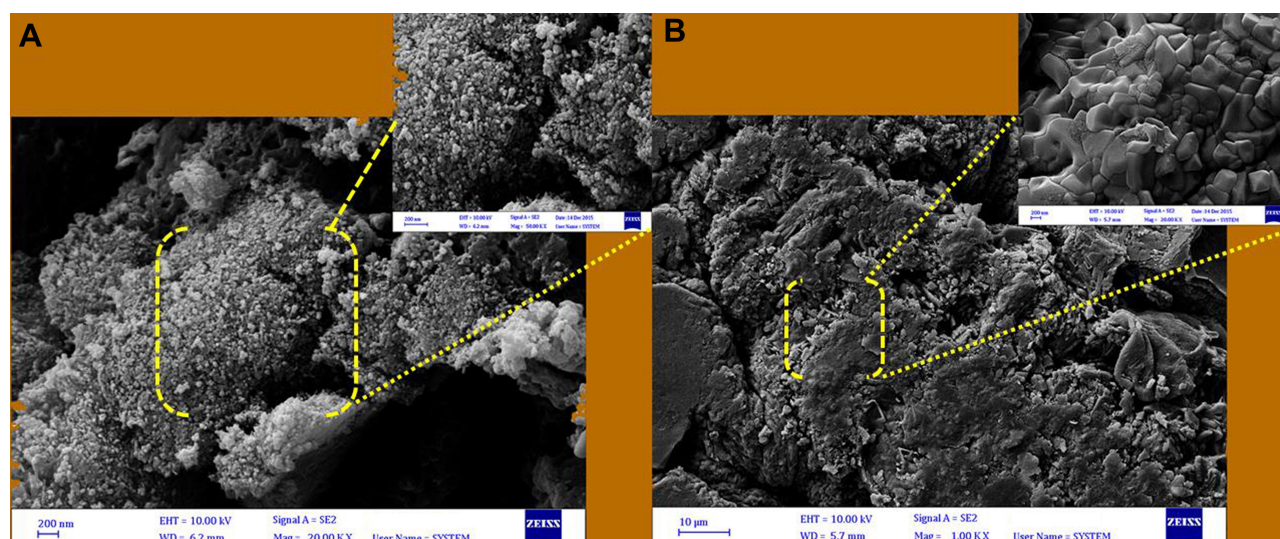


**Figure 2** SEM micrographs of the synthesized particles: **(A)** CS/β-CD/TPP-Folic acid/Alg and **(B)** CS/β-CD/TPP-Folic acid/Alg-CUR.

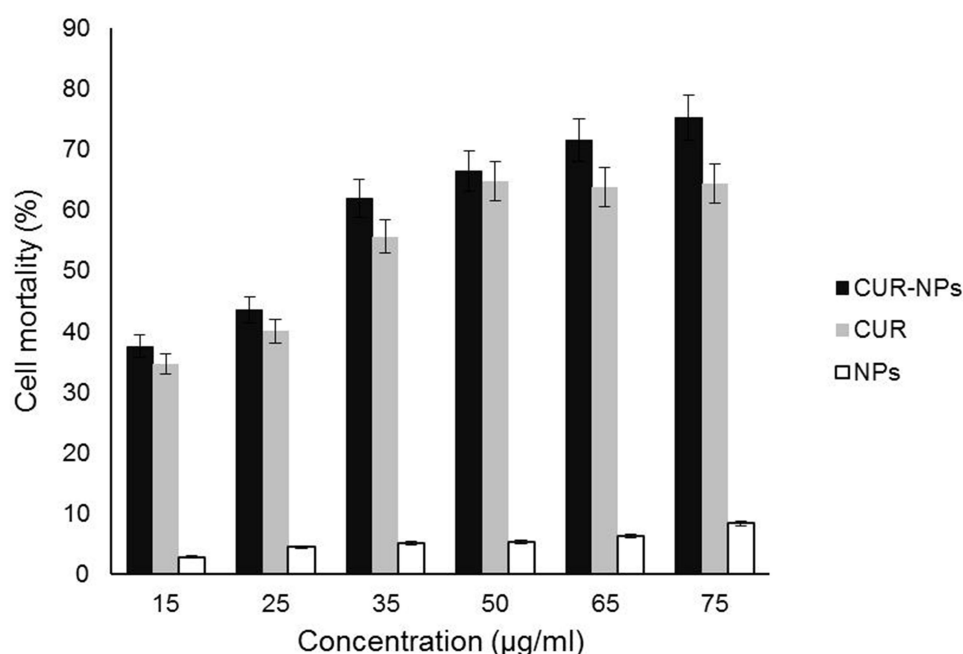


**Figure 3** Cytotoxicity effect of CUR (Curcumin), NPs (CS/β-CD/TPP-Folic acid/Alg) and CUR-NPs (CS/β-CD/TPP-Folic acid/Alg-CUR) on the KMBC-10 spheroids cells.

clinical applications such as side effects, limited absorption, and fast metabolism.<sup>32</sup> On the other hand, similar results were represented that curcumin loaded nanoparticles including chitosan could greatly improve the enhancement of uptake of curcumin in comparison to the cytotoxicity of curcumin loaded nanoparticles, which was not also observed cytotoxic effect than unmodified curcumin in some doses.<sup>33</sup> Furthermore, research showed that the cellular uptake of curcumin was more effective by encapsulated curcumin

into polymers in carcinoma cells.<sup>34</sup> Other reports obtained showed that adding of PEG into chitosan hydrochloride (CSH)-hyaluronic acid (HA) nanoparticles improved circulation of drug nanocarriers in blood and permeability in tumors.<sup>35</sup> Studies showed that CUR-PNPs exhibited stronger cytotoxicity than the curcumin solution in rat glioma cells.<sup>35</sup> The folic acid-chitosan nanoparticles enhanced circulation time, drug solubility and improved uptake in tumors and also hydrophobic drugs conjugate stronger with folate-chitosan

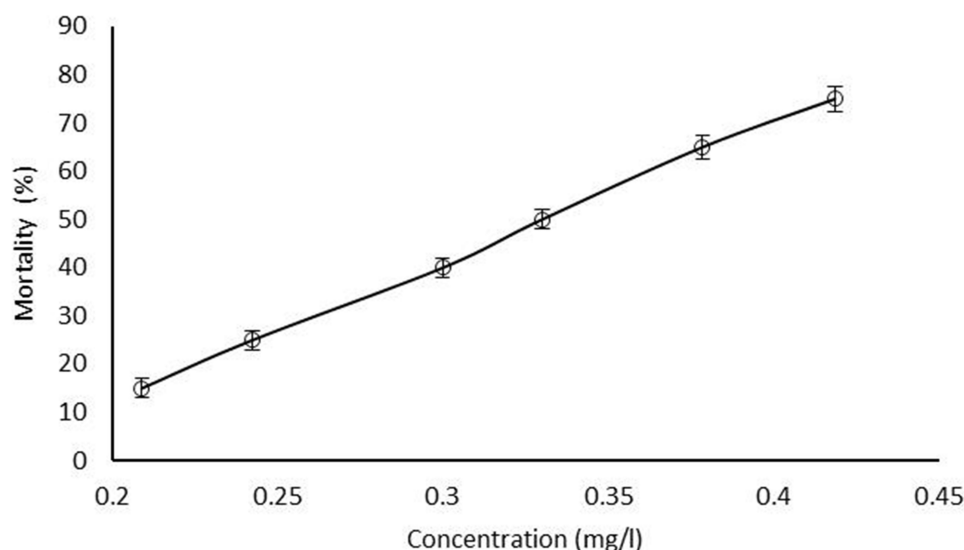


**Figure 4**  $IC_{50}$  values of the CS/β-CD/TPP-Folic acid/Alg-CUR against KMBC-10 spheroids cells.

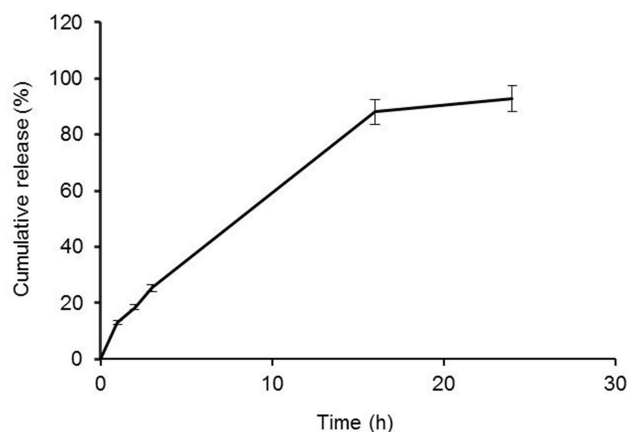


**Figure 5** Release profile of curcumin from CS/β-CD/TPP-Folic acid/Alg nano-spheres through dialysis membrane into PBS (pH 5.8) as receiver medium.

nano capsules via hydrophobic contacts and van der Waals.<sup>36</sup> Also, a majority of the apoptotic cells were observed when folate-modified nano complex used as drug delivery systems instead of the non-folate-modified nano complex.<sup>37</sup> In another study, folate receptors were used to enhance the specificity of the gold nanoparticles by tailoring folic acid on their surface.<sup>38</sup> CUR-loaded nanomicells play a role more efficient in expression of epithelial-mesenchymal transition (EMT) markers than curcumin free.<sup>32</sup>

According to the recent results, curcumin-loaded PLGA NPs coated with chitosan and PEG can efficiently increase anti-invasive property, cytotoxicity, apoptosis compared to curcumin alone.<sup>39</sup> Chitosan nanoparticles more efficient attachment onto cancer cells and PEG nanoparticles may

prevent the phagocytosis process. Moreover, these nanoparticles enhance drug pharmacokinetics in blood.<sup>40</sup> Similar results obtained about apoptosis show that curcumin in chitosan-coated poly (butyl) cyanoacrylate nanoparticles are able to make better necrosis and also apoptosis in HepG2 cells compared to free curcumin.<sup>41</sup> In another study, curcumin was encapsulated in positively charged nanoparticles to deliver curcumin into the negatively charged carcinoma cells. Besides, it is mainly important to increase solubility and cell cytotoxicity.<sup>6</sup> Alginate was used to synthesize the hydrogels that are hydrophilic to conjugate with hydrophobic anticancer drugs. For example, gold nanoparticles as photothermal agents and alginate hydrogels were used to enable concurrent thermo-chemotherapy.<sup>42,43</sup> Recent findings indicated that curcumin loaded polyelectrolyte complex (PEC) nanoparticles prepared from cationically modified gelatin and sodium alginate (Alg) were suitable complex for delivery of curcumin to carcinoma cells MCF-7.<sup>9</sup> Results of the injection of curcumin in rats were in agreement with similar research demonstrating that curcumin alone after intravenous administration was quickly removed from the blood stream, compared with CUR/nanospheres. However, carriers are able to effectively avoid rapid clearing of curcumin from the blood.<sup>35</sup> Previous study confirmed that the folic acid interaction with the chitosan by H-bonding and van der Waals contacts and these are utilized for delivery in vitro, while we investigated this contact by FTIR analysis.<sup>22</sup> Cell culture techniques were divided into 2 and 3 dimensional (2D and 3D) environment that showed an essential role on the cells



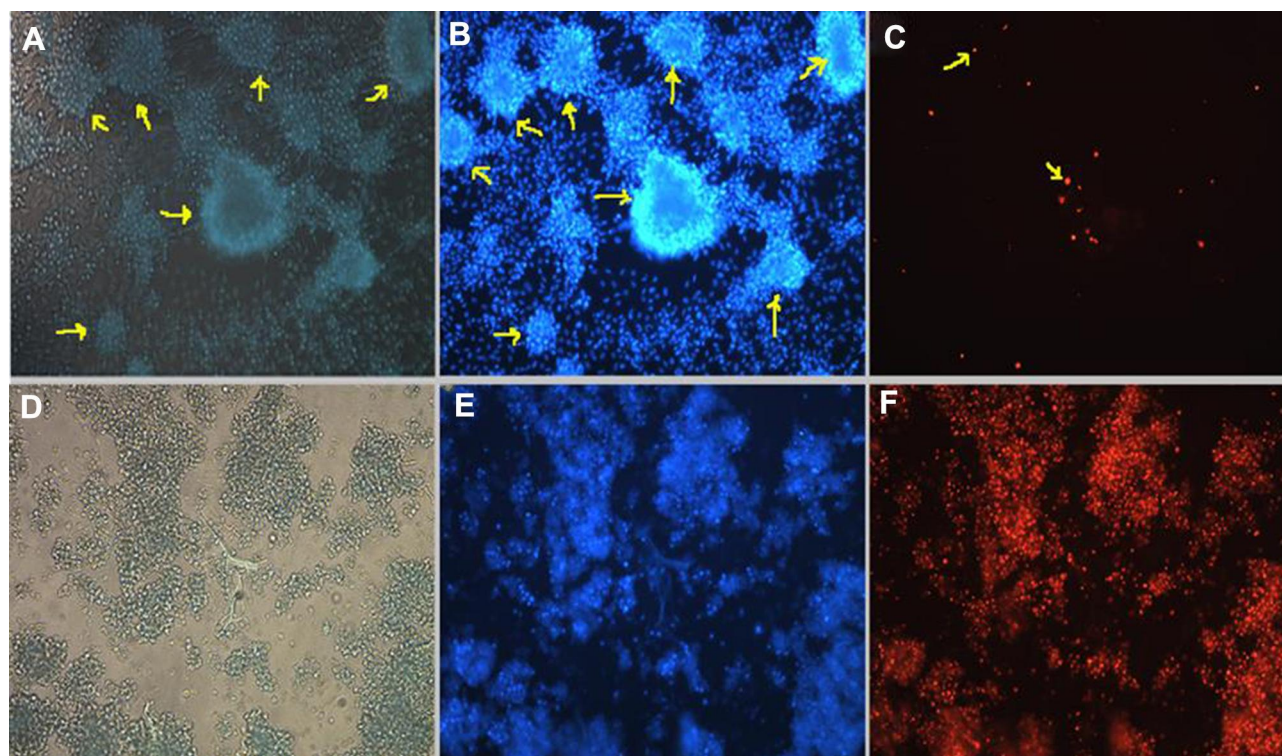


**Figure 6** KMBC-10 spheroids cells treated with curcumin and CS/β-CD/TPP-Folic acid/Alg-CUR nanospheres and then stained by Hoechst 33,258 (H) and PI staining (40 x, final magnification). (A) Optical microscope, (B) Hoechst staining and (C) PI staining micrographs of KMBC-10 spheroids cells treated with curcumin, respectively. (D) Optical microscope, (E) Hoechst staining and (F) PI staining micrographs of KMBC-10 spheroids cells treated with CS/β-CD/TPP-Folic acid/Alg-CUR nanospheres, respectively. The red cells represent dead cells, while the blue cells indicate live cells.

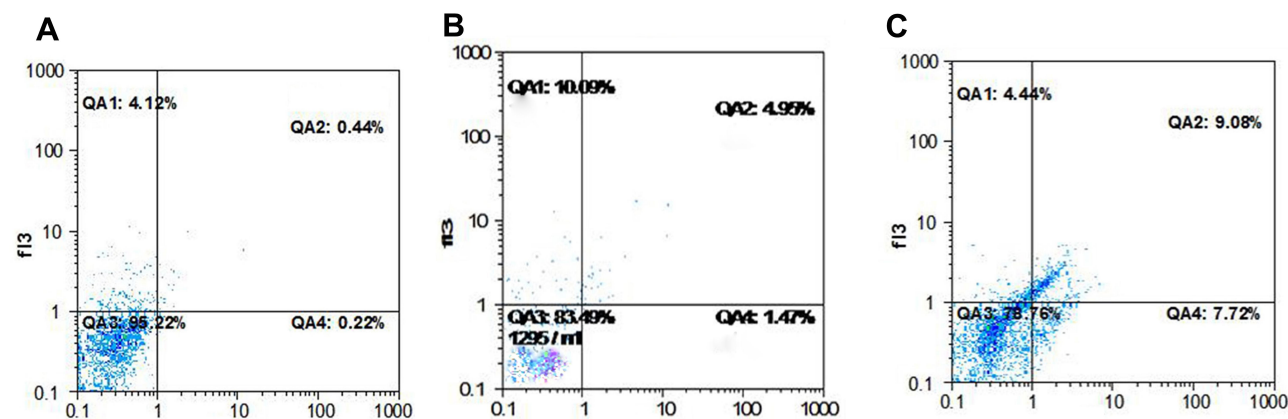


**Figure 7** Apoptotic assay on the KMBC-10 spheroids cells treated by (A) CS/β-CD/TPP-Folic acid/Alg, (B) Curcumin and (C) CS/β-CD/TPP-Folic acid/Alg-CUR was analyzed by Annexin V-FITC/PI staining and flow cytometry.

fate and their behavior.<sup>44</sup> 2D cell culture is used mostly in cancer research even with all its limitations.<sup>45</sup> Because of these limitations, scientists were led to create a model that is as similar as in vivo conditions. Thereafter, attention was drawn to 3D cell culture, because of more physiological similarities to in vivo tests.<sup>46</sup> 3D cell culture is done as cell spheroids/aggregated on matrix or embedded within matrix,

or scaffold-free cell spheroids in suspension.<sup>47</sup> Fibrin scaffolds were applied to differentiate mesenchymal stem cells in the previous studies.<sup>48–51</sup> Scaffold-free cell spheroids in suspension are generated by floating methods include forced and hanging drop method. For example, various culture conditions were used to differentiate human umbilical cord matrix-derived mesenchymal stem cells (hUCMs) into insulin



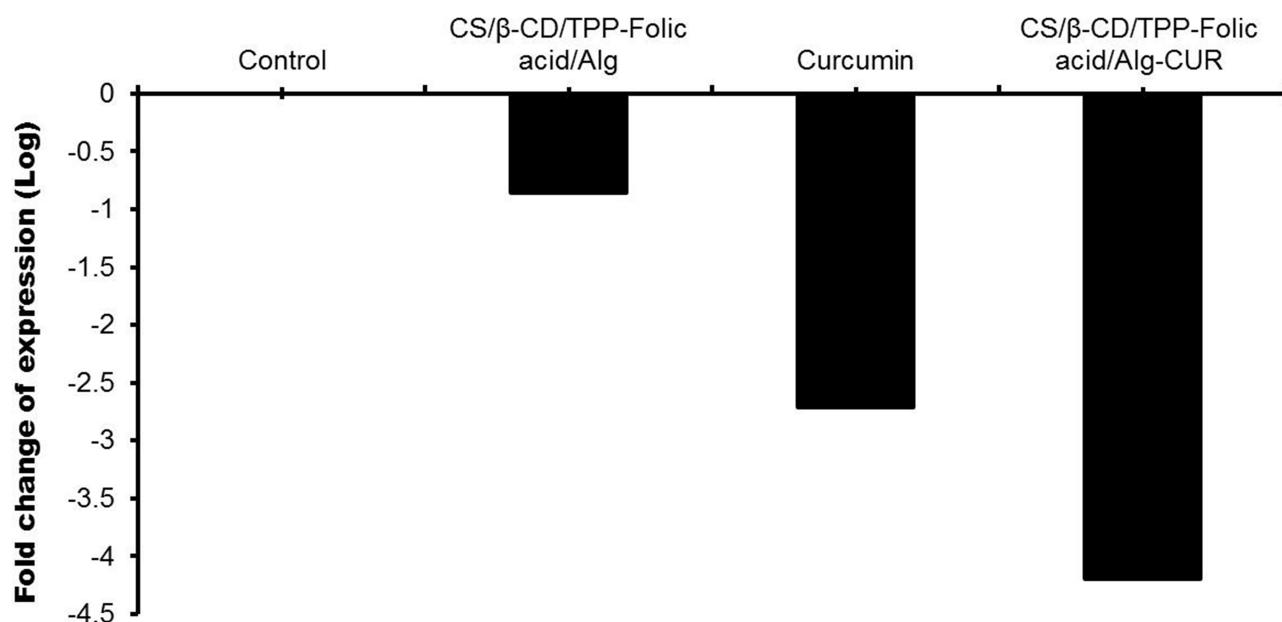


**Figure 8** Evaluation of *CXCR4* gene expressions level on KMBC-10 spheroids cells that were treated with CS/β-CD/TPP-Folic acid/Alg-CUR and CS/β-CD/TPP-Folic acid/Alg and curcumin. *CXCR4* gene expressions level was decreased in treatment group (CS/β-CD/TPP-Folic acid/Alg-CUR) compared to curcumin and controls.

production cells.<sup>52</sup> Results showed that the production of the insulin was more in hanging drop culture compared to 2D cell culture. In the present study, forced floating methods was conducted to have a suspension culture. Paclitaxel loaded cyclodextrin nanospheres play an important role of the anticancer activity in 3D multicellular spheroids MCF-7 and following on drug delivery system was investigated in vivo studies as described previously.<sup>53</sup> Previous reports were indicated that expression of *CXCR4* in the cancer cells was enhanced.<sup>54</sup> Curcumin-loaded CS-ALG-TPP NPs strongly decreased the apoptotic gene expression (*Bax*) and also significantly decreased the anti-apoptotic gene expression (*Bcl2*) compared with carrier and free curcumin.<sup>55</sup>

## Conclusion

According to the release profile's graph, it could be concluded that the high amount of curcumin was loaded on the CS/β-CD/TPP-Folic acid/Alg nanospheres, and released slowly during 24 h. Moreover, it is also obvious that the absorption of the curcumin by spheroids was highly effective because of more reasons. First of all, using 3D cell culture that creates the environment the same as in vivo in which cells are permitted to grow and interact with their surroundings. Secondly, folic acid that exists on the nanospheres could ligand with folate receptors and uptake the nanospheres inside the spheroids. In addition, apoptotic mostly occurred in the treated spheroids by targeted nanospheres, while the treated spheroids

by curcumin showed necrosis. Proliferation in the treated cells by targeted nanospheres was significantly less than that obtained by the traditional delivery system.

## Acknowledgment

This research received no specific grant from any funding agency in the public. The author would like to have a special thanks to Kerman University of Medical Sciences because of its spiritual and ethical support.

## Disclosure

The authors report no conflicts of interest in this work.

## References

1. Reynolds DS, Tevis KM, Blessing WA. Breast cancer spheroids reveal a differential cancer stem cell response to chemotherapeutic treatment. *Sci Rep*. 2017;7(1):10382. doi:10.1038/s41598-017-10863-4
2. Youlten DR, Cramb SM, Dunn NA, Muller JM, Pyke CM, Baade PD. The descriptive epidemiology of female breast cancer: an international comparison of screening, incidence, survival and mortality. *Cancer Epidemiol*. 2012;36(3):237–248. doi:10.1016/j.canep.2012.02.007
3. Dhumal DM, Kothari PR, Kalhapure RS, Akamanchi KG. Self-microemulsifying drug delivery system of curcumin with enhanced solubility and bioavailability using a new semi-synthetic bicephalous heterolipid: in vitro and in vivo evaluation. *RSC Adv*. 2015;5(110):90295–90306. doi:10.1039/C5RA18112G
4. Salem M, Rohani S, Gillies ER. Curcumin, a promising anti-cancer therapeutic: a review of its chemical properties, bioactivity and approaches to cancer cell delivery. *RSC Adv*. 2014;4(21):10815–10829. doi:10.1039/c3ra46396f

5. Ntoutoume GMN, Granet R, Mbakidi JP, et al. Development of curcumin-cyclodextrin/cellulose nanocrystals complexes: new anticancer drug delivery systems. *Bioorg Med Chem.* **2016**;26(3):941–945. doi:10.1016/j.bmc.2015.12.060
6. Popat A, Karmakar S, Jambhunkar S, Xu C, Yu C. Curcumin-cyclodextrin encapsulated chitosan nanoconjugates with enhanced solubility and cell cytotoxicity. *Colloids Surf B Biointerfaces.* **2014**;117:520–527. doi:10.1016/j.colsurfb.2014.03.005
7. Zainuddin N, Ahmad I, Kargarzadeh H, Ramli S. Hydrophobic kenaf nanocrystalline cellulose for the binding of curcumin. *Carbohydr Polym.* **2017**;163:261–269. doi:10.1016/j.carbpol.2017.01.036
8. Li J, Mooney DJ. Designing hydrogels for controlled drug delivery. *Nat Rev Mater.* **2016**;1(12):16071.
9. Sarika P, James NR. Polyelectrolyte complex nanoparticles from cationised gelatin and sodium alginate for curcumin delivery. *Carbohydr Polym.* **2016**;148:354–361. doi:10.1016/j.carbpol.2016.04.073
10. Liu J, Xu L, Liu C, et al. Preparation and characterization of cationic curcumin nanoparticles for improvement of cellular uptake. *Carbohydr Polym.* **2012**;90(1):16–22. doi:10.1016/j.carbpol.2012.04.036
11. Song W, Su X, Gregory DA, Li W, Cai Z, Zhao X. Magnetic alginate/chitosan nanoparticles for targeted delivery of curcumin into human breast cancer cells. *Nanomaterials.* **2018**;8(11):907. doi:10.3390/nano8110907
12. Ghaz-Jahanian MA, Abbaspour-Aghdam F, Anarjan N, Berenjian A, Jafarizadeh-Malmiri H. Application of chitosan-based nanocarriers in tumor-targeted drug delivery. *Mol Biotechnol.* **2015**;57(3):201–218. doi:10.1007/s12033-014-9816-3
13. Darini A, Eslaminejad T, Mahani SNN, Ansari M. Magnetogel nanoparticles composed of cisplatin-loaded alginate/b-cyclodextrin as controlled release drug delivery. *Adv Pharm Bull.* **2019**;9(4):571–577. doi:10.15171/apb.2019.065
14. Douzandeh Mobarrez B, Ansari Dogaheh M, Eslaminejad T, Kazemipour M, Shakibaie M. Preparation and evaluation the antibacterial effect of magnetic nanoparticles containing gentamicin: a preliminary in vitro study. *Iran J Biotechnol.* **2018**;16:287–293. doi:10.21859/ijb.1559
15. Afzali E, Forootanfar H, Eslaminejad T, Amirpour-Rostami S, Ansari M. Enhancing purification of  $\alpha$ -amylase by superparamagnetic complex with alginate/chitosan/ $\beta$ -cyclodextrin/TPP. *Biocatalysis Biotransformation.* **2019**;37(3):201–209.
16. Eslaminejad T, Nouredin Nematollahi-Mahani S, Ansari M. Glioblastoma targeted gene therapy based on pEGFP/p53-loaded superparamagnetic iron oxide nanoparticles. *Curr Gene Ther.* **2017**;17(1):59–69. doi:10.2174/1566523217666170605115829
17. Eslaminejad T, Nematollahi-Mahani SN, Ansari M. Synthesis, characterization, and cytotoxicity of the plasmid EGFP-p53 loaded on pullulan-spermine magnetic nanoparticles. *JMMM.* **2016**;402:34–43. doi:10.1016/j.jmmm.2015.11.037
18. Mazzotta E, De Benedittis S, Qualtieri A, Muzzalupo R. Actively targeted and redox responsive delivery of anticancer drug by chitosan nanoparticles. *Pharmaceutics.* **2020**;12(1):26. doi:10.3390/pharmaceutics12010026
19. Vedagiri H, Jenifer MH, Mirulalini GS. Integrative analysis of CXCR4/CXCL12 axis gene expression alterations in breast cancer and its prognostic relevance. *Gene Rep.* **2018**;11:6–11. doi:10.1016/j.genrep.2018.01.007
20. Eslaminejad T, Nematollahi-Mahani SN, Ansari M. Cationic  $\beta$ -cyclodextrin-chitosan conjugates as potential carrier for pmcherry-cl gene delivery. *Mol Biotechnol.* **2016**;58(4):287–298. doi:10.1007/s12033-016-9927-0
21. Mahmoud KA, Mena JA, Male KB, Hrapovic S, Kamen A, Luong JH. Effect of surface charge on the cellular uptake and cytotoxicity of fluorescent labeled cellulose nanocrystals. *ACS Appl Mater Interfaces.* **2010**;2(10):2924–2932. doi:10.1021/am1006222
22. Chanphai P, Konka V, Tajmir-Riahi H. Folic acid-chitosan conjugation: A new drug delivery tool. *J Mol Liq.* **2017**;238:155–159. doi:10.1016/j.molliq.2017.04.132
23. Liu X, Chen X, Li Y, Wang X, Peng X, Zhu W. Preparation of superparamagnetic Fe<sub>3</sub>O<sub>4</sub>@ alginate/chitosan nanospheres for Candida rugosa lipase immobilization and utilization of layer-by-layer assembly to enhance the stability of immobilized lipase. *ACS Appl Mater Interfaces.* **2012**;4(10):5169–5178. doi:10.1021/am301104c
24. Pillai JJ, Thulasidasan AKT, Anto RJ, Devika NC, Ashwanikumar N, Kumar GV. Curcumin entrapped folic acid conjugated PLGA-PEG nanoparticles exhibit enhanced anticancer activity by site specific delivery. *RSC Adv.* **2015**;5(32):25518–25524. doi:10.1039/C5RA00018A
25. Perche F, Patel NR, Torchilin VP. Accumulation and toxicity of antibody-targeted doxorubicin-loaded PEG-PE micelles in ovarian cancer cell spheroid model. *J Controlled Release.* **2012**;164(1):95–102. doi:10.1016/j.jconrel.2012.09.003
26. Khoobi M, Khalilvand-Sedagheh M, Ramazani A, Asadgol Z, Forootanfar H, Faramarzi MA. Synthesis of polyethyleneimine (PEI) and  $\beta$ -cyclodextrin grafted PEI nanocomposites with magnetic cores for lipase immobilization and esterification. *J Chem Technol Biotechnol.* **2014**.
27. Gazori T, Khoshayand MR, Azizi E, Yazdizade P, Nomani A, Haririan I. Evaluation of Alginate/Chitosan nanoparticles as antisense delivery vector: formulation, optimization and in vitro characterization. *Carbohydr Polym.* **2009**;77(3):599–606. doi:10.1016/j.carbpol.2009.02.019
28. Sharpe LA, Daily AM, Horava SD, Peppas NA. Therapeutic applications of hydrogels in oral drug delivery. *Expert Opin Drug Deliv.* **2014**;11(6):901–915. doi:10.1517/17425247.2014.902047
29. Murugadoss S, Brassinne F, Sebaihi N, et al. Agglomeration of titanium dioxide nanoparticles increases toxicological responses in vitro and in vivo. *Part Fibre Toxicol.* **2020**;17(1):10. doi:10.1186/s12989-020-00341-7
30. Tahara K, Sakai T, Yamamoto H, Takeuchi H, Kawashima Y. Establishing chitosan coated PLGA nanosphere platform loaded with wide variety of nucleic acid by complexation with cationic compound for gene delivery. *Int J Pharm.* **2008**;354(1–2):210–216. doi:10.1016/j.ijpharm.2007.11.002
31. Yang R, Yang S-G, Shim W-S, et al. Lung-specific delivery of paclitaxel by chitosan-modified PLGA nanoparticles via transient formation of microaggregates. *J Pharm Sci.* **2009**;98(3):970–984. doi:10.1002/jps.21487
32. Dagrada G, Rupel K, Zacchigna S, et al. Self-assembled nanomicrospheres as curcumin drug delivery vehicles: impact on solitary fibrous tumor cell protein expression and viability. *Mol Pharm.* **2018**;15(10):4689–4701. doi:10.1021/acs.molpharmaceut.8b00655
33. Mohanty C, Sahoo SK. The in vitro stability and in vivo pharmacokinetics of curcumin prepared as an aqueous nanoparticulate formulation. *Biomaterials.* **2010**;31(25):6597–6611. doi:10.1016/j.biomaterials.2010.04.062
34. Nasery MM, Eslaminejad T, Mandeghary A, et al. Cytotoxicity evaluation of curcumin-loaded affibody-decorated liposomes against breast cancerous cell lines. *J Liposome Res.* **2020**. 1–20. doi:10.1080/08982104.2020.1755981
35. Xu Y, Asghar S, Yang L, et al. Nanoparticles based on chitosan hydrochloride/hyaluronic acid/PEG containing curcumin: in vitro evaluation and pharmacokinetics in rats. *Int J Biol Macromol.* **2017**;102:1083–1091. doi:10.1016/j.ijbiomac.2017.04.105
36. Chanphai P, Thomas T, Tajmir-Riahi H. Design of functionalized folic acid-chitosan nanoparticles for delivery of tetracycline, doxorubicin, and tamoxifen. *J Biomol Struct Dyn.* **2018**;1–7.
37. Montazerabadi A, Beik J, Irajirad R, et al. Folate-modified and curcumin-loaded dendritic magnetite nanocarriers for the targeted thermo-chemotherapy of cancer cells. *Artif Cells Nanomed Biotechnol.* **2019**;47(1):330–340. doi:10.1080/21691401.2018.1557670

38. Zeinizada E, Tabei M, Shakeri-Zadeh A, et al. Selective apoptosis induction in cancer cells using folate-conjugated gold nanoparticles and controlling the laser irradiation conditions. *Artif Cells Nanomed Biotechnol.* 2018;46(sup1):1026–1038. doi:10.1080/21691401.2018.1443116
39. Arya G, Das M, Sahoo SK. Evaluation of curcumin loaded chitosan/PEG blended PLGA nanoparticles for effective treatment of pancreatic cancer. *Biomed Pharmacother.* 2018;102:555–566. doi:10.1016/j.biopha.2018.03.101
40. Perrault SD, Walkey C, Jennings T, Fischer HC, Chan WC. Mediating tumor targeting efficiency of nanoparticles through design. *Nano Lett.* 2009;9(5):1909–1915. doi:10.1021/nl900031y
41. Duan J, Zhang Y, Han S, et al. Synthesis and in vitro/in vivo anti-cancer evaluation of curcumin-loaded chitosan/poly (butyl cyanoacrylate) nanoparticles. *Int J Pharm.* 2010;400(1–2):211–220. doi:10.1016/j.ijpharm.2010.08.033
42. Alamzadeh Z, Beik J, Pirhajati Mahabadi V, et al. Ultrastructural and optical characteristics of cancer cells treated by a nanotechnology based chemo-photothermal therapy method. *J Photochem Photobiol B: Biol.* 2019;192:19–25. doi:10.1016/j.jphotobiol.2019.01.005
43. Mirrahimi M, Abed Z, Beik J, et al. A thermo-responsive alginate nanogel platform co-loaded with gold nanoparticles and cisplatin for combined cancer chemo-photothermal therapy. *Pharmacol Res.* 2019;143:178–185. doi:10.1016/j.phrs.2019.01.005
44. Kapalczyńska M, Kolenda T, Przybyła W, et al. 2D and 3D cell cultures - a comparison of different types of cancer cell cultures. *Archives Medical Sci.* 2018;14(4):910–919.
45. Duval K, Grover H, Han L-H, et al. Modeling Physiological Events in 2D vs. 3D Cell Culture. *Physiology.* 2017;32(4):266–277.
46. Antoni D, Burckel H, Josset E, Noel G. Three-dimensional cell culture: a breakthrough in vivo. *Int J Mol Sci.* 2015;16(3):5517–5527. doi:10.3390/ijms16035517
47. Chaicharoenaudomrung N, Kunhorm P, Noisa P. Three-dimensional cell culture systems as an in vitro platform for cancer and stem cell modeling. *WJSC.* 2019;11(12):1065–1083. doi:10.4252/wjsc.v11.i12.1065
48. Seyed F, Farsinejad A, Nematollahi-Mahani SN. Fibrin scaffold enhances function of insulin producing cells differentiated from human umbilical cord matrix-derived stem cells. *Tissue Cell.* 2017;49(2):227–232. doi:10.1016/j.tice.2017.03.001
49. Bagheri-Hosseinabadi Z, Mesbah-Namin SA, Salehinejad P, Seyed F. Fibrin scaffold could promote survival of the human adipose-derived stem cells during differentiation into cardiomyocyte-like cells. *Cell Tissue Res.* 2018;372(3):571–589. doi:10.1007/s00441-018-2799-9
50. Bagheri-Hosseinabadi Z, Seyed F, Mollaei HR, Moshrefi M, Seifalian A. Combination of 5-azaytidine and hanging drop culture convert fat cell into cardiac cell. *Biotechnol Appl Biochem.* 2020. doi:10.1002/bab.1897
51. Najafipour H, Bagheri-Hosseinabadi Z, Eslaminejad T, Mollaei HR. The effect of sodium valproate on differentiation of human adipose-derived stem cells into cardiomyocyte-like cells in two-dimensional culture and fibrin scaffold conditions. *Cell Tissue Res.* 2019;378(1):127–141. doi:10.1007/s00441-019-03027-5
52. Seyed F, Farsinejad A, Nematollahi-Mahani SA, Eslaminejad T, Nematollahi-Mahani SN. Suspension culture alters insulin secretion in induced human umbilical cord matrix-derived mesenchymal cells. *Cell J.* 2016;18(1):52–61.
53. Varan G, Patrulea V, Borchard G, Bilensoy E. Cellular interaction and tumoral penetration properties of cyclodextrin nanoparticles on 3d breast tumor model. *Nanomaterials.* 2018;8(2):67. doi:10.3390/nano8020067
54. Nobutani K, Shimono Y, Mizutani K, et al. Downregulation of CXCR4 in metastasized breast cancer cells and implication in their dormancy. *PLoS One.* 2015;10(6):e0130032. doi:10.1371/journal.pone.0130032
55. Ahmadi F, Ghasemi-Kasman M, Ghasemi S, et al. Induction of apoptosis in HeLa cancer cells by an ultrasonic-mediated synthesis of curcumin-loaded chitosan-alginate-sTPP nanoparticles. *Int J Nanomed.* 2017;12:8545. doi:10.2147/IJN.S146516

## International Journal of Nanomedicine

### Publish your work in this journal

The International Journal of Nanomedicine is an international, peer-reviewed journal focusing on the application of nanotechnology in diagnostics, therapeutics, and drug delivery systems throughout the biomedical field. This journal is indexed on PubMed Central, MedLine, CAS, SciSearch®, Current Contents®/Clinical Medicine,

Submit your manuscript here: <https://www.dovepress.com/international-journal-of-nanomedicine-journal>

Journal Citation Reports/Science Edition, EMBase, Scopus and the Elsevier Bibliographic databases. The manuscript management system is completely online and includes a very quick and fair peer-review system, which is all easy to use. Visit <http://www.dovepress.com/testimonials.php> to read real quotes from published authors.